wind radiation damage, which is over two orders of magnitude greater than estimates based on the buildup of solar wind–implanted species, such as Ar and He (*15*). Our data support the conclusions of Kerridge and Kaplan (*16*), who suggested that the effective sputtering rate on the lunar surface is slowed by the simultaneous accumulation of impact-generated vapors.

If amorphous rims result from radiation damage (*1–4*), then the rims should be compositionally the same as their hosts. However, the compositional differences observed in this study, combined with the distribution of Fe particles in the rims, indicates that solar wind radiation damage is not the major mechanism for the formation of amorphous rims. Solar wind damage can have, at most, a minor effect. It has been suggested that the ancient solar wind was not as active as the contemporary wind, on the basis of the thickness of the amorphous rims and assumptions regarding the exposure history of individual soil grains on the lunar surface (*4*); this conclusion is not valid.

Hapke *et al.* (*14*) showed that experimental vapor coatings produced by vapor deposition and sputtered ion deposition are dark and have optical properties that resemble those of the lunar fines. Hapke also showed that sputtering of lunar fines produces the requisite darkening. In all these cases, it seems that the most important ingredient is the presence of submicroscopic Fe metal grains, which are strong absorbers of visible wavelengths. The presence of fine-grained Fe metal in the amorphous rims could also contribute to the darkening process, but it is not yet known if there is a sufficient concentration of Fe particles to have a significant effect.

Theoretical work indicates that considerable amounts of vapor should be produced during micrometeorite impacts into the lunar regolith and that much of the vapor must recondense onto nearby soil grains (*17, 18*). However, questions remain regarding the fate of impact-generated vapors because no petrographically distinct vapor-deposited material had been identified in lunar soils. Despite a considerable body of evidence that the surfaces of lunar fines are enriched in some elements relative to the bulk soil (*19–22*), there has been no consensus on the degree of enrichment or on the mechanism responsible for the surface enrichments. Our study shows that vapor deposits are present in the lunar regolith as thin amorphous rims on soil grains. The main characteristics of these condensates are an enrichment in volatile elements (particularly Si and S), a marked depletion in refractory elements, and Fe in the form of metallic particles on the order of nanometers in size. Contributions to these amorphous coatings by sputtered iron deposition and radiation damage are probably of minor importance relative to the contribution of direct condensation of impact-generated vapors.

REFERENCES AND NOTES

1. J. C. Dran *et al.*, *Earth Planet. Sci. Lett.* **9**, 391 (1970).
2. J. Bibring *et al.*, *Science* **175**, 753 (1972).
3. M. Maurette and P. B. Price, *ibid.* **187**, 121 (1975).
4. J. Borg *et al.*, in *The Ancient Sun: Fossil Record in the Earth, Moon, and Meteorites*, R. O. Pepin, J. A. Eddy, R. B. Merrill, Eds. (Pergamon, New York, 1980), p. 431.
5. Aliquots of the <20-μm size fraction of each soil were embedded in low-viscosity epoxy, and thin sections ~100 nm thick were prepared by diamond knife ultramicrotomy. The EDX analyses were collected so that counting statistics errors for major elements were <1%; relative errors associated with the determination of experimental *k* factors are <5%. Microtome thin sections of the soils were analyzed using a JEOL 2000FX TEM equipped with a LINK EDX spectrometer. Probe sizes were typically 30 to 40 nm, less than the apparent thickness of the amorphous rims. Multiple analyses of individual rims fall within the analytical uncertainties of the EDX technique.
6. C. E. Rees and H. G. Thode, *Proc. Lunar Planet. Sci. Conf.* **5**, 1963 (1974).
7. J. D. Cripe and C. B. Moore, *ibid.* **7**, 469 (1976).
8. G. DeMaria *et al.*, *ibid.* **2**, 1367 (1971).
9. A. V. Ivanov and K. P. Florensky, *ibid.* **6**, 1341 (1975).
10. M. T. Naney *et al.*, *ibid.* **7**, 155 (1976).
11. L. P. Keller and D. S. McKay, *Lunar Planet. Sci.* **XXII**, 137 (1992).
12. A. E. Potter and T. H. Morgan, *Science* **241**, 675 (1988).
13. O. I. Yakovlev *et al.*, *Geokhimiya* **12**, 1698 (1988).
14. B. Hapke *et al.*, *Moon* **13**, 339 (1975).
15. J. F. Kerridge, *Lunar Planet. Sci. Conf.* **XXI**, 301 (1991).
16. ——— and I. R. Kaplan, *ibid.* **9**, 1687 (1978).
17. H. A. Zook, *ibid.* **6**, 1653 (1975).
18. M. J. Cintala, *J. Geophys. Res.* **97**, 947 (1992).
19. B. Hapke *et al.*, in *Proceedings of the Apollo 11 Lunar Science Conference*, A. A. Levinson, Ed. (Pergamon, New York, 1970), p. 2199.
20. T. Gold *et al.*, *Proc. Lunar Planet. Sci. Conf.* **7**, 901 (1976).
21. R. M. Housley and R. W. Grant, *ibid.*, p. 881.
22. E. Zinner *et al.*, *ibid.* **9**, 1667 (1978).

23. This work supported by NASA RTOP 152-17-40-21. We thank H. Zook for a review of an early version of the manuscript.

22 April 1993; accepted 2 July 1993

Lattice Effect of Strong Electron Correlation: Implication for Ferroelectricity and Superconductivity

T. Egami,* S. Ishihara, M. Tachiki

Much theoretical work has been devoted to understanding the role of strong electron correlations in high-temperature superconductivity mainly through magnetic interactions, but the possible role of electron correlation in ferroelectricity of metal oxides has not received attention. Diagonalization of a simple many-body, tight-binding Hamiltonian shows that the electron-lattice interaction is dramatically enhanced in some cases by strong electron correlation because of deformation-induced charge transfer. This effect may be closely related to ferroelectricity and superconductivity in transition metal oxides.

High-temperature superconductors are doped Mott insulators, such as $La_{2-x}Sr_xCuO_4$. In the Mott insulator, conduction is inhibited by strong electron-electron correlation, which does not allow two carriers to be on the same lattice site. One consequence of strong electron correlation is the spin polarization of an atom, and much theoretical attention in high-temperature superconductivity has focused on the effect of magnetic interactions (*1, 2*). In comparison, there has been relatively little discussion of the effect of electron correlation on the electron-lattice interaction. Even less has been written about the possible role of electron correlation in ferroelectricity, although superconducting oxides are close in composition and structure to ferroelectric oxides and there is a possible connection (*3, 4*). We suggest that strong electron correlation can have a significant effect on the electron-lattice interaction with some drastic consequences in certain situations, and this could have profound implications for the mechanism of ferroelectricity and possibly of high-temperature superconductivity.

The origin of ferroelectricity in transition metal oxides such as $BaTiO_3$ is usually discussed in terms of ionic displacements and the internal Lorentz field produced by the polarization. However, the inadequacy of such a simple view has been known for a long time (*5*), and the need to take the covalency of the bond into account has been advocated. A recent local density approximation (LDA)–linearized augmented plane wave (LAPW) calculation on $BaTiO_3$ (*6*) demonstrates the importance of covalency in ferroelectric po-

Institute for Materials Research, Tohoku University, Sendai 980, Japan.

*Also in the Department of Materials Science and Engineering and the Laboratory for Research on the Structure of Matter, University of Pennsylvania, Philadelphia, PA 19104–6272.

larization. That calculation showed that, even though the valence of Ti is 4+ and the d state has no electrons (d^0) in the purely ionic picture, the actual valence of Ti is less than 3+ with the d^1 configuration because of dp hybridization (6). Recent photoemission studies support this view (7, 8). A calculation on $KNbO_3$ and $KTaO_3$ (9) also suggests strong hybridization. Thus, there is a distinct possibility that the electron correlation is important in these solids.

We start with a simple tight-binding model for a binary compound, AB, with an average of one electron per site. We think of A as a transition metal element (Ti) and B as oxygen. We assume that (i) the difference in site energy, $\Delta = E_A - E_B$, is positive to model the relative energy levels of Ti and O, (ii) the electron hopping is only between the nearest neighbors, AB, and (iii) the electron correlation is described by the on-site Hubbard term with U_A and U_B, the local correlation energies, which are significant and comparable in magnitude with Δ. The Hamiltonian of the system is

$$H = t\sum_{i,j,\sigma} c^+_{A,i,\sigma}c_{B,j,\sigma} + \Delta\sum_{i,\sigma} c^+_{A,i,\sigma}c_{A,i,\sigma} + U_A\sum_i n_{A,i,\uparrow}n_{A,i,\downarrow} + U_B\sum_j n_{B,j,\uparrow}n_{B,j,\downarrow} + \text{H.C.} \quad (1)$$

where t is the transfer matrix between sites A and B, i and j are nearest neighbors, c^+ and c are the electron creation and annihilation operators, respectively, $n = c^+c$, σ denotes spin ($\Uparrow\Downarrow$), H.C. stands for Hermite conjugate, and we assume $E_B = 0$. When Δ is much larger than t, U_A, and U_B, there are two electrons at each B site and no electrons at the A site. We assume that in this state, the ionic limit, the compound is chemically described as $A^{2+}B^{2-}$, in an obvious association with a transition metal oxide, $M^{2+}O^{2-}$.

Because Δ was chosen to be positive, the upper Hubbard band of A is always nearly empty. Consequently, the value of U_A has little effect on electron occupation as long as it is reasonably large. If we assume that t is small compared with U_A, U_B, and Δ, it is immediately obvious that when $U_B > \Delta$, the system is a Mott-Hubbard type insulator, in the sense that the electron correlation is dominant with nearly one electron at each site. On the other hand, if U_B is smaller, the system is an ionic insulator with nearly two electrons on each B site (Fig. 1). Therefore, by modifying the value of U_B or Δ, one can induce a major charge transfer between A and B. Indeed, a very similar phenomenon of crossover from a neutral insulator to an ionic solid was observed for low-dimensional organic systems (10), and there is a theory describing this transition (11).

The role of the transfer matrix t is merely to modify this balance quantitatively as long as the lattice is perfectly periodic. However, when the lattice is deformed, there is a qualitative change in the phenomena. The lattice deformation can result in the change of both t and Δ; the latter is attributable to the change in the Madelung energy. When the state of the system is between a Mott insulator and an ionic insulator, lattice deformation can trigger substantial charge transfer from one atom to the other. This is the basis of the strong electron-lattice interaction instigated by the strong electron correlation.

To illustrate this point, we carried out a many-electron calculation on the Hamiltonian (Eq. 1) for a one-dimensional ring made of 4A and 4B sites and eight electrons. (As for the parameters in Eq. 1, we chose dimensionless values which would be reasonable in the unit of electron volt to describe the light transition metal oxides.) The many-body Hamiltonian was exactly diagonalized by the modified Lanczos method (12) for the basis set of $4^8 = 65{,}536$ states. The results obtained for the smaller system of 3A and 3B sites were similar, indicating that the relatively small size of the model does not significantly affect the conclusion, particularly because the system is insulating. Calculations on a larger system are computationally inhibiting at present.

For fixed values of t and Δ, the average number of electrons occupying the A site, N_A, jumps from about 0.6 to about 0.8 as the value of U_B is increased (Fig. 2). Clearly, the system is making an abrupt transition from an ionic insulator with some covalency to the Mott insulator. The ionic-covalent band state, which may be approximated by a single electron band, abruptly changes to the Mott-Hubbard state. Close to this transition, it is difficult to achieve convergence of the calculation because two eigenstates are nearly degenerate. The abruptness of the transition is not at all eased by the increase in the value of t. The effect of t is merely to modify the crossover point. In general, the transfer t works against the correlation energy U, so that when t is increased, the crossover occurs at larger values of U_B. There is a small difference in the position of the crossover point between the larger 4A + 4B system and the smaller 3A + 3B system (Fig. 2), but the overall behavior does not depend on the size of the system. This jump must be essentially the same as the one observed for organic materials (10, 11).

We then modified the lattice by assuming a Brillouin-zone boundary phonon, thus introducing dimerization. The system is now a chain of AB molecules (AB-AB-AB- . . .). To represent the effect of this dimerization, we changed the value of t alternatingly by $\pm\Delta t$ (13). However, we kept Δ constant for the sake of simplicity. This caused a decrease in the ground-state energy, which is quadratic in Δt for small values of Δt. The effect is present even when U_A and U_B are zero because dimerization increases the band gap between the occupied and unoccupied bands. This instability against dimerization in the case of $\Delta = U_A = U_B = 0$ is the well-known Peierls instability. Because we did not include the atom-atom repulsion, the ground-state energy is maximum at $\Delta t = 0$. When the repulsion is included, the total energy has a minimum or minima. If the repulsion is stronger than the decrease in the band energy, dimerization does not occur. But if it is weaker, the total energy is minimum at a finite value of Δt. Because the state with $-\Delta t$ will be symmetrically related, the ground state will be doubly degenerate, resulting in the double-well state.

The effect of electron correlation on the decrease in the ground-state energy is evident in a plot of the change in the ground-state energy $\Delta E(U_B)$ for a fixed value of Δt

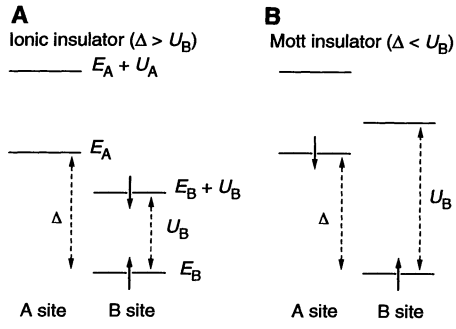

Fig. 1. Electronic-level scheme of the compound AB with the difference in the single-site energy, Δ, and the local correlation energies, U_A and U_B. (**A**) When $\Delta > U_B$, the system is an ionic insulator, whereas (**B**) if $\Delta < U_B$, it is a Mott-Hubbard insulator.

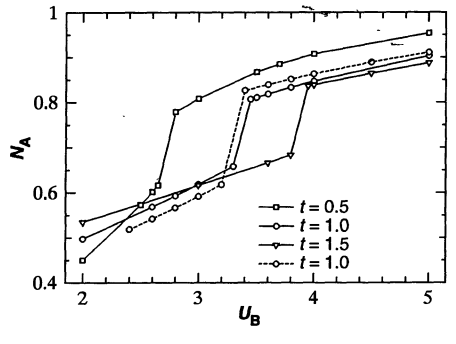

Fig. 2. Dependence of N_A on U_B for $\Delta = 2$ and $U_A = 5$ for various values of t. Results are shown for both the 4A + 4B system (solid lines) and the 3A + 3B system (dashed line).

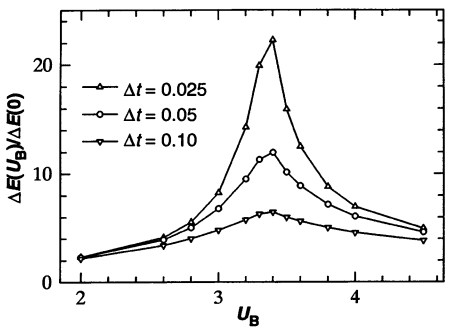

Fig. 3. Change in the ground-state energy, $\Delta E(U_B)$, of the Hamiltonian (Eq. 1) as a result of dimerization, normalized to the value for $U_B = 0$ for various values of Δt. We assumed $t = 1$ and $U_A = 5$.

(Fig. 3). The ratio, $\Delta E(U_B)/\Delta E(0)$, which describes the degree of enhancement of the electron-lattice interaction by electron correlation, shows a sharp maximum at the value of U_B that corresponds to the crossover point. This result demonstrates clearly that the electron-lattice interaction is very significantly enhanced by electron correlation, particularly in the vicinity of the crossover point, and the enhancement can amount to more than an order of magnitude, depending on the values of U_B and Δt.

We found that the first-order nature of the transition from the Mott-Hubbard state to the ionic state disappears as soon as dimerization is introduced. When Δt is nonzero, the value of N_A as a function of U_B shows a rapid but continuous change through the transition region. At the same time, the weight of the local spin-singlet, or valence bond, state, as in a hydrogen molecule (Heitler-London state), changes rapidly with the value of Δt. The weight of this valence bond state can be measured by the nearest neighbor spin-spin correlation function

$$K_{AB} = \langle\langle S_{A,i} \cdot S_{Bj} \rangle\rangle \qquad (2)$$

where $S_{A,i}$ is the spin of the atom i at site A. In the spin-singlet state on an isolated pair, $K_{AB} = -3/4$. The ground state has a significant component of the spin-singlet state in the Mott-Hubbard state ($K \approx -0.3$), as expected, and less in the ionic state. Even when the value of U_B is not at the crossover point, dimerization induces rapid changes in K_{AB}. Dimerization increases the spin correlation within the pair and decreases the interpair spin correlation, both of which contribute to the increase in the local spin-singlet component within the pair. The formation of a local valence bond state induces a large change in the ground state energy and significant charge transfer from A to B, or vise versa; this is the origin of this strong lattice effect.

The effect of strong electron correlation on the electron-lattice interaction was studied for a one-band Hubbard model, in relation to the Peierls distortion in one-dimensional conductors such as polyacetylene (*14, 15*). Some enhancement attributable to the formation of the valence bond state was found, but the amount of enhancement was very slight, only about 20%, because the formation of the valence bond was not coupled to charge transfer. This electron-lattice interaction accompanied by charge transfer cannot be described by the conventional deformation potential and calls for a description that is highly nonlinear. Phenomenologically, this description can be modeled by the nonlinear interaction (*16*) but, as shown above, the interaction critically depends on the parameters involved and cannot be described by a single-atom potential.

There are important implications for the present result. First, the propensity for dimerization described above is possibly the origin of ferroelectricity in the transition metal oxides that undergo displacive transformation. In particular the amount of local charge strongly depends on Δt in the neighborhood of the crossover point (Fig. 4). The sense of the change is such that if the value of U_B is hypercritical and the system is in the Mott-Hubbard state (N_A close to unity), electrons are transferred by dimerization from A atoms to B atoms; thus, the ionicity, or the local charge polarization, is increased. This enhances ferroelectricity when the Coulomb interaction between ions is considered. On the other hand, if the value of U_B is subcritical, electrons move from B to A upon dimerization; thus, the ionicity is reduced, and ferroelectricity is suppressed by the long-range Coulomb interaction. Therefore, strong ferroelectricity is expected in a Mott insulator close to the crossover condition rather than in the ionic side. These effects of intersite Coulomb interaction will be discussed elsewhere (*17*).

The role of the nonlinear electron-lattice interaction in ferroelectricity was already phenomenologically discussed by Bilz *et al.* (*18, 19*), and the importance of electronic interactions for ferroelectricity has long been known and was recently demonstrated by Cohen and Krakauer (6). However, the LDA used in their LAPW calculation does not fully represent the effect of strong electron correlation because the many-body nature of the spin correlation is not properly included. Thus, it is likely that the effect of correlation is grossly underestimated. More importantly, the physics of the effect of electron correlation is buried in the full potential calculations. The present model calculation, albeit in oversimplification, demonstrates the dramatic effect of electron correlation.

Second, the present calculation suggests that it is necessary to reexamine the role that the electron-lattice interaction plays in the high-temperature superconductivity of oxides. High-temperature superconductivity occurs in the vicinity of the crossover point in composition from a Mott-Hubbard insulator to a band metal. Although our calculations have been performed only for insulators and the introduction of carriers may lead to some moderation of the sharp transition by screening, we feel that the mechanism described above should still apply at least qualitatively to the transition from a Mott-Hubbard insulator to a metal.

The possibility of strong electron correlation affecting the nature of the electron-lattice interaction in superconducting oxides was discussed recently by Yonemitsu *et al.* (*20*) in a slightly different context. They focused on the stability of the Zhang-Rice singlet state in the σ^* band made of Cu-$d_{x^2-y^2}$ and O-$p_{x,y}$. Therefore, in that case, the electron correlation at the oxygen site, U_p, apparently is not playing a major role. On the other hand, the effect of U_p is critically important in our case. Therefore, our study applies better, for instance, to the case of the A_{1g} states composed of Cu-d_{z^2} and O-p_z states, where the magnitude of U_p is comparable with the bandwidth. Thus, the nonlinearity of the electron-lattice coupling discussed in relation to the double-well state of the apical oxygen (*21*) is more closely related.

Various possible scenarios in which this new electron-lattice interaction brings about the superconductivity can be considered, including the multiband Bardeen-Cooper-Schrieffer (BCS) superconductivity

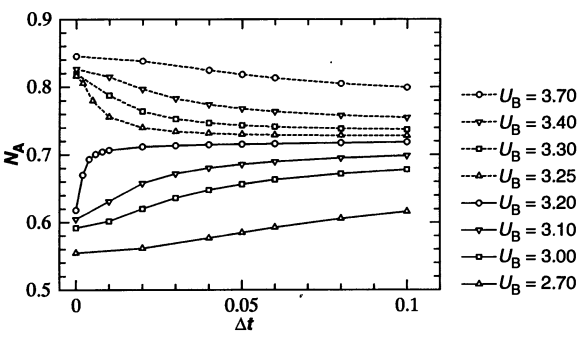

Fig. 4. Electron density on site A, N_A, as a function of Δt for various values of U_B. We assumed $\Delta = 2$, $t = 1$, and $U_A = 5$. The result in this figure is for the 3A + 3B system. Note that large values of N_A, close to unity, correspond to the Mott-Hubbard state, and small values, below 0.6, are found in the ionic state.

(*22*) and the bipolaron-mediated two-component superconductivity (*23, 24*). In particular, deformation-induced charge transfer could provide the mechanism for a polaron mostly dressed by electron and thus having a small mass (*25*). More extensive studies of this nonlinear electron-lattice coupling could lead to a better understanding of the effect of electron correlation on various properties of oxides including ferroelectricity and superconductivity.

REFERENCES AND NOTES

1. P. W. Anderson, *Science* **235**, 1196 (1987).
2. F. C. Zhang and T. M. Rice, *Phys. Rev. B* **37**, 3759 (1988).
3. A. R. Bishop, R. L. Martin, K. A. Müller, Z. Tesanovic, *Z. Phys. Sect. B* **76**, 17 (1989).
4. S. K. Kurtz, J. R. Hardy, J. W. Flocken, *Ferroelectrics* **87**, 29 (1988).
5. A. R. von Hippel, *J. Phys. Soc. Jpn.* **28** (suppl.), 1 (1970).
6. R. E. Cohen and H. Krakauer, *Phys. Rev. B* **42**, 6416 (1990).
7. L. T. Hudson, R. L. Kurtz, S. W. Robey, D. Temple, R. L. Stockbauer, *ibid.* **47**, 1174 (1993).
8. A. Fujimori, personal communication.
9. T. Neumann, G. Borstel, C. Scharfschwerdt, M. Neumann, *Phys. Rev. B* **46**, 10623 (1992).
10. J. B. Torrance, J. E. Vazquez, J. J. Mayerle, V. Y. Lee, *Phys. Rev. Lett.* **46**, 253 (1981).
11. J. Hubbard and J. B. Torrance, *ibid.* **47**, 1750 (1981).
12. E. Dagotto and A. Moreo, *Phys. Rev. D* **31**, 865 (1985).
13. W. P. Su, J. R. Schrieffer, A. J. Heeger, *Phys. Rev. B* **22**, 2099 (1980).
14. S. Mazumdar and S. N. Dixit, *Phys. Rev. Lett.* **51**, 292 (1983).
15. J. E. Hirsch, *ibid.*, p. 296.
16. A. Bussmann-Holder, H. Buttner, A. Simon, *Phys. Rev. B* **39**, 207 (1989).
17. S. Ishihara, T. Egami, M. Tachiki, in preparation.
18. H. Bilz, G. Benedek, A. Bussmann-Holder, *Phys. Rev. B* **35**, 4840 (1987).
19. A. Bussmann-Holder, H. Bilz, G. Benedek, *ibid.* **39**, 9214 (1989).
20. K. Yonemitsu, A. R. Bishop, J. Lorenzana, *Phys. Rev. Lett.* **69**, 965 (1992).
21. J. Mustre-de Leon *et al.*, *ibid.* **68**, 3236 (1992).
22. A. Bussmann-Holder, in preparation.
23. R. Micnas, J. Ranninger, S. Robaszkiewicz, *Rev. Mod. Phys.* **62**, 113 (1990).
24. Y. Bar-Yam, *Phys. Rev. B* **43**, 359 (1991); *ibid.*, p. 2601.
25. J. E. Hirsch, *ibid.* **47**, 5351 (1993).

26. We are grateful to R. E. Cohen, A. Bussmann-Holder, A. Fujimori, Y. Ohta, S. Maekawa, E. Mele, H. Matsumoto, T. Koyama, and S. Takahashi for useful discussions. Supported by the Ministry of Education, Science, and Culture, Japan (Grant-in-Aid), the Office of Naval Research (N00014-91-J-1036), and the National Science Foundation (DMR90-01704 and DMR91-20668).

20 May 1993; accepted 28 July 1993

Molecular Dynamics of Adsorption and Segregation from an Alkane Mixture

T. K. Xia and Uzi Landman

Adsorption and segregation of *n*-hexadecane molecules from an equal by weight mixture of *n*-hexadecane and *n*-hexane to an Au(001) surface at 315 kelvin are studied with the use of molecular dynamics simulations. Preferential adsorption of *n*-hexadecane at the solid-to-liquid interface together with subsequent layer-by-layer growth of an ordered, wetting interface were observed. The long chains penetrate and adsorb at the interfacial layer by means of a sequential segmental mechanism involving end-segment anchoring and displacive desorption of preadsorbed *n*-hexane molecules.

The dynamic, thermodynamic, structural, and compositional properties of liquids and liquid mixtures can be significantly modified by surfaces and by confinement to narrow pores or films (*1–6*). In particular, surface segregation, or preferential adsorption, of long-chain molecules from a homologous polymer mixture of long- and short-chain components is a commonly observed phenomenon that is of considerable interest (*2–6*). Applications include adhesion, lubrication, colloidal stability and flocculation, chromatographic separation, the properties of plasticized polymeric materials (for which the concentration of the plasticized or reinforcing filler at the surface may be different from that in the interior), and the biocompatibility of artificial internal organs.

Whereas the kinetics and chain-length dependence of adsorption and wetting from polymer mixtures have been investigated extensively (*3–9*), issues pertaining to the dynamics of such processes are rather complex and have only recently been addressed experimentally and theoretically (*3*). Computer-based modeling and simulations open new avenues for investigation of the structure, energetics, and dynamics of complex liquids, as well as other materials systems (*10–13*). We report results of large-scale molecular dynamics (MD) simulations of surface segregation from an initially homogeneous alkane mixture (*14, 15*)—*n*-hexadecane (n-$C_{16}H_{34}$) and *n*-hexane (n-C_6H_{14})—which exhibits preferential adsorption of the long-chain molecules, occurring by means of a layer-by-layer epitaxial wetting. Furthermore, the simulations reveal that the atomic-scale dynamical adsorption mechanism involves sequential, segmental, reptation-like penetration and adsorption processes. Such a mechanism has been proposed and discussed recently in the context of experimental studies of adsorption-desorption kinetics of polymer chains at a solid surface (*3, 4, 7*).

In the MD simulations, which consist of the integration of the Newtonian equations of motion, we have investigated a 1:1 (by weight) mixture of *n*-hexane (400 molecules) and *n*-hexadecane (150 molecules), modeled with use of alkane interaction potentials, including dihedral, bond-angle, and nonbonded interactions. These potentials have been tested and used successfully in previous studies of bulk and interfacial liquid alkane systems (*11, 16–18*). The interactions between the CH_2 and CH_3 segments of the alkane molecules and a static crystalline Au(001) surface were modeled (*11, 17*) with 6-12 Lennard-Jones (LJ) potentials, where the parameters were fitted to experimentally estimated desorption data (the same segmental adsorption energy was assumed for both molecules). The strength of the interaction between a molecular segment and a gold atom is three times larger than that of the nonbonded intersegment interaction (*11, 17, 19*). The calculational cell, whose dimensions in the x and y directions, parallel to the solid surface, were 61.2 Å, was replicated in these directions with periodic boundary conditions; however, no periodicity was applied along the normal (z) direction.

In the first stage of the simulation, the mixture was prepared by means of a procedure described previously (*11*) that involved prolonged ($>10^3$ ps) equilibration of a homogeneous free mixture at a high temperature (450 K) followed by the cooling and adsorption of the mixture to form a liquid film at 315 K, which is above the melting temperature of either of the two components (291 and 178 K for the C_{16} and C_6 alkanes, respectively) but below their boiling points. The simulations were performed in the canonical (isothermal) ensemble, with infrequent thermalization by means of the scaling of particle velocities. The equations of motion were integrated with a 5th order predictor-corrector algorithm (*13*), with a time step $\Delta t = 3.86 \times 10^{-15}$ s, and the preferential adsorption process was simulated for 8 ns.

The total segmental density profile (ρ_s) (Fig. 1A, solid line) was calculated at the end of the simulation and exhibits density oscillations corresponding to interfacial layering of the film next to the solid-liquid interface, together with a tailing of the density at the liquid-vapor interface (*11*). The segmental density-difference profile

School of Physics, Georgia Institute of Technology, Atlanta, GA 30332.